NASA Technical Memorandum

NASA TM - 103516

COALIGNED OBSERVATIONS OF SOLAR MAGNETIC FIELDS AT DIFFERENT HEIGHTS—MSFC CENTER DIRECTOR'S DISCRETIONARY FUND FINAL REPORT (PROJECT 88-10)

By M.J. Hagyard, E.A. West, G.A. Gary, and J.E. Smith

Space Science Laboratory
Science and Engineering Directorate

September 1990

National Aeronautics and Space Administration

George C. Marshall Space Flight Center

TABLE OF CONTENTS

LIST OF ILLUSTRATIONS

LIST OF ILLUSTRATIONS

TECHNICAL MEMORANDUM

COALIGNED OBSERVATIONS OF SOLAR MAGNETIC FIELDS AT DIFFERENT HEIGHTS - MSFC CENTER DIRECTOR'S DISCRETIONARY FUND FINAL REPORT

(Project Number 88-10)

1. INTRODUCTION

The interaction of magnetic fields and plasmas is a common process throughout the universe, and it is the controlling force in the dynamic, high-energy phenomena observed on the Sun. The origin, evolution, and development of the Sun's magnetic field to produce these energetic processes are central themes in today's solar research, and extensive observational studies are carried out to develop an understanding of just how the solar magnetic field plays this key role in solar activity.

MSFC has a unique instrument for observing the Sun's magnetic field, the MSFC Solar Vector Magnetograph [1-3]. Using this instrument, MSFC scientists have made many significant contributions over the past decade to an understanding of the magnetic Sun, with the result that MSFC is recognized worldwide as a leader in the study of solar magnetic fields.

Because the instrument obtains measurements in only one spectral line of the optical spectrum from the Sun, the MSFC Solar Vector Magnetograph provides maps of the solar magnetic field at only one level in the solar atmosphere, the photosphere. There are certain limitations to observing at only this one height; obviously, it would be advantageous to have measurements at two different heights. For example, there are many phenomena that take place above the photosphere. Prominences are cool, dense sheets of solar plasma that are suspended far above the photosphere, rising into the solar corona to heights of 50,000 km. They are readily visible in some chromospheric spectral images, particularly in the Hα line, but are invisible at the photosphere. We believe that the solar magnetic field must somehow provide the supporting mechanism that maintains this dense plasma in its less dense surroundings. Yet measurements of the photospheric field provide information only on the underlying magnetic field; we need to visualize how that field is configured at the heights of the prominence to understand how it supports the prominence material and to understand what happens to that supporting field when a prominence erupts upward, sometimes leaving the Sun entirely.

The solar flare is another example of a solar phenomenon that occurs at heights in the solar atmosphere above the regions where the MSFC magnetograph measures the field. Indeed, except in the rare event of a "white-light" flare, most flares have no observable effect at the photospheric level; they initiate in the corona and produce observable emission only down to chromospheric levels. However, even though the flare itself occurs above the photosphere, the photospheric magnetic field is very much involved in the flare process. As an active region grows and evolves, stresses in the coronal magnetic field build up in response to changes in the field at the photospheric level caused by sunspot motions and emerging flux. It is the free energy of these stressed fields that is believed to be the source of energy for flares. To understand the

flare phenomenon, therefore, we must understand the processes by which this energy is built up, stored, and then released, so that the magnetic field, from photosphere to corona, is the key physical quantity to be known. Observations that give us measurements of the field at the photosphere and chromosphere would provide at least part of the overall picture, especially the connectivity of the field in the chromosphere with its roots in the photosphere below.

Some information about fields higher up can be gained by extrapolating the observed photospheric field upward, but the numerical techniques used to do this depend on various theoretical models that involve making some assumptions about the field. Usually, the assumptions are not altogether realistic and are made solely to make the mathematical analysis tractable. Thus there may be doubts as to how well the model represents the actual field configuration above the photosphere. By having observations that show the configuration of the magnetic field at a higher level, we can compare the observed chromospheric field with the field extrapolated from a given model and thus gain insight into the applicability of that particular model.

Recognizing the benefits of observing the structure and evolution of the Sun's magnetic field at two different heights in the solar atmosphere, MSFC scientists have enhanced the research capabilites of the MSFC Solar Vector Magnetograph by coaligning an Hα telescope with the magnetograph's telescope. In this manner we obtain coaligned and cotemporal images of the photospheric vector field and the morphology of the chromospheric field. The capabilities are further enhanced by incorporating image-processing hardware so that coaligned time-lapse movies of the two fields can be studied.

In this report we describe the project undertaken to carry out this modification to the MSFC magnetograph. In Section 2, a description of the two instruments is presented, and the method used for coaligning the telescopes is described in Section 3. The system developed for image processing is outlined in Section 4, and some initial results are presented in Section 5. The paper concludes with a summary section.

2. DESCRIPTION OF THE MAGNETOGRAPH AND Hα TELESCOPE

The MSFC Solar Observatory is located at the Marshall Space Flight Center in Huntsville, Alabama. The Observatory's facilities consist of the vector magnetograph located on the top of a 40-foot steel tower, a 12.5-cm Razdow Hα telescope housed at the base of the tower in a metal dome, an 18-cm Questar telescope with a full aperture white-light filter, and a 30-cm Cassegrain telescope, located in a second metal dome, that is to become a second experimental vector magnetograph in the near future. A building at the base of the tower provides office space, darkroom and optical test facilities, workshop, and computer facilities for data analysis.

The MSFC vector magnetograph is a unique instrument, one of only a few worldwide that measure all three components of the magnetic field on the Sun. The telescope is an f/13, 30-cm Cassegrainian system that focuses a 3.5-cm image of the Sun on a mirrored aperture stop. This stop limits the field-of-view of the transmitted image to 5.7 x 5.7 arcminute, about the size

of typical active regions. Polarizing optics, a 1/8 Å bandpass spectral filter, and a 320 x 512 pixel CCD camera are sealed in a steel optics "box" that is attached to the back end of the telescope. Operation of the magnetograph is controlled entirely by an Intel microprocessor; the microprocessor is in turn controlled via a programmable minicomputer data system consisting of a PDP 11-23 computer, disk drives, tape unit, and terminal. This computer system is linked to the data analysis computer system consisting of a PDP 11-73 and a μVax 3500, tape units, disk drives, optical disk, printers, array processor, and terminals.

The Hα telescope that was chosen for coalignment with the MSFC magnetograph was the backup unit for the Skylab ATM Hα 1 telescope [4]. This 16.5-cm aperture telescope consisted of a telecentric Cassegrainian objective (f/28), Fabry-Perot filter, relay optics, vidicon camera, and film camera. A heat-rejection optical window assembly was mounted in front of the telescope aperture to reduce internal heating. The dielectric coatings on the window selectively transmitted 65% of the energy at the Hα wavelength within a 300-Å half power bandwidth while rejecting 95% of the solar energy in the spectral region from 3900 Å to the far IR. The heat rejection window was shown to reduce the internal solar heat load from 47 W to 2.5 W.

The system provided a variable field of view (4.4 - 16 arcminute), narrow spectral bandwidth (0.7 Å), and high spatial resolution (1.5 arcsecond for the 4.4 arcminute field-of-view). Since a Fabry-Perot filter's spectral response is sensitive to variations in the angle of incidence, the telecentric system was chosen so that the exit pupil is placed at infinity. This configuration maintains constant cone and chief ray angles at the plane of the Fabry-Perot filter located just to the rear of the Cassegrainain focal plane. As a result, uniform spectral characteristics are maintained across the 16-arcminute field-of-view.

A 5.1-cm image of the Sun is formed at the Cassegrainian focal plane. In the original design, this image was relayed to one of two image planes - the vidicon or film camera - via a zoom lens and a fixed relay lens, respectively. We have modified these optics, removing the film camera and replacing it with an eyepiece for direct viewing. Also, we have replaced the vidicon with a solid state CCD camera while retaining the zoom relay lens that provides fields of view ranging from 4.4 to 16 arcminute.

The Fabry-Perot filter provides a relatively large aperture and high transmission at the wavelength of the Hα spectral line, 6562.8 Å. The filter is housed in a thermally controlled oven to maintain it at the required operating temperature and thereby keep it spectrally tuned. The filter is a solid-etalon device, consisting of a substrate and a stack of alternate quarter-wave layers of high and low index materials constituting the first mirror element. A thin piece of fused silica (about 100 μm thick) is placed on top of this dielectric stack and covered with a second mirror stack of high and low index material. A 7 Å (full width at half maximum) prefilter is used to block the unwanted transmission peaks produced at 11 Å intervals by this etalon.

The instrument was designed to be controlled from the ATM control panel on Skylab. We thus had to design our own control panel to operate the thermal controller, zoom lens, and telescope focus. When this controller had been fabricated, we tested the telescope and filter

using a heliostat to feed a solar image into the system. We found that the telescope and filter were in exceptionally good condition after being in storage for about 16 years, and we obtained very good quality images of the Sun in Hα. The only flaws were some scratches on the telecentric lens; since this lens is very near the prime focus, the scratches were very evident in the CCD images. We therefore obtained the specifications for this lens and have procured and installed a new one.

3. DESIGN OF THE COALIGNMENT MECHANISM

There were three primary considerations in developing the method for coaligning the two telescopes. First, it was essential to minimize the added weight so as not to exceed the capability of the Ealing telescope mounting and drive system (shown in Figure 1). This pier-mounted system was designed to support only the vector magnetograph instrument. However, preliminary calculations indicated that it could accommodate the added weight of the ATM Hα telescope if the two telescopes were properly balanced when mounted together. Thus, this requirement for achieving a well-balanced, dual-telescope system was the second major consideration. The third consideration was to achieve a method for precise adjustments of one telescope with respect to the other after they had been attached so that an accurate coalignment could be achieved.

The weight and balance considerations were really interrelated problems. After being mounted on the drive system, the dual-telescope system would eventually be balanced by adding appropriate counterweights, and the counterweights needed would be determined by the location of the center of gravity of the dual-telescope system with respect to the pivot point where the telescopes are mounted to the drive system. After excess parts of the Hα telescope were removed, centers of gravity were determined for both the Hα telescope and the vector magnetograph. Also, designs were generated for the large mounting bracket that would hold the two telescopes and be attached to the Ealing drive. Two linear positioning stages were designed to be attached to the mounting bracket between the two telescopes; these would provide movement of the Hα telescope relative to the magnetograph in two axes for alignment purposes. These designs and the data on the centers of gravity provided the input for a computer program to determine the positioning of the telescopes on the mounting bracket that would place the center of gravity of the total system at the pivot point where the telescopes mounted to the Ealing drive. The final design determined by this method is shown in Figure 2.

After fabrication of the necessary parts, the system was integrated and the coaligned dual-telescope instrument was realized. Front and rear views of the dual system are shown in Figures 3 and 4, respectively. In Figure 5, the coaligned telescopes are seen mounted to the Ealing drive at the observing site.

The added weight of the Hα telescope does impose an extra load on the Ealing tracking system, but we have operated the dual system over a period of 10 months and have not encountered any major problems associated with the tracking system. We have determined that care must be exercised in the support of the heavy cabling that connects electronics in the vector magnetograph's optics box with the microprocessor; any large imbalance caused by shifts of

Vector Magnetograph Telescope Mounting and Drive System

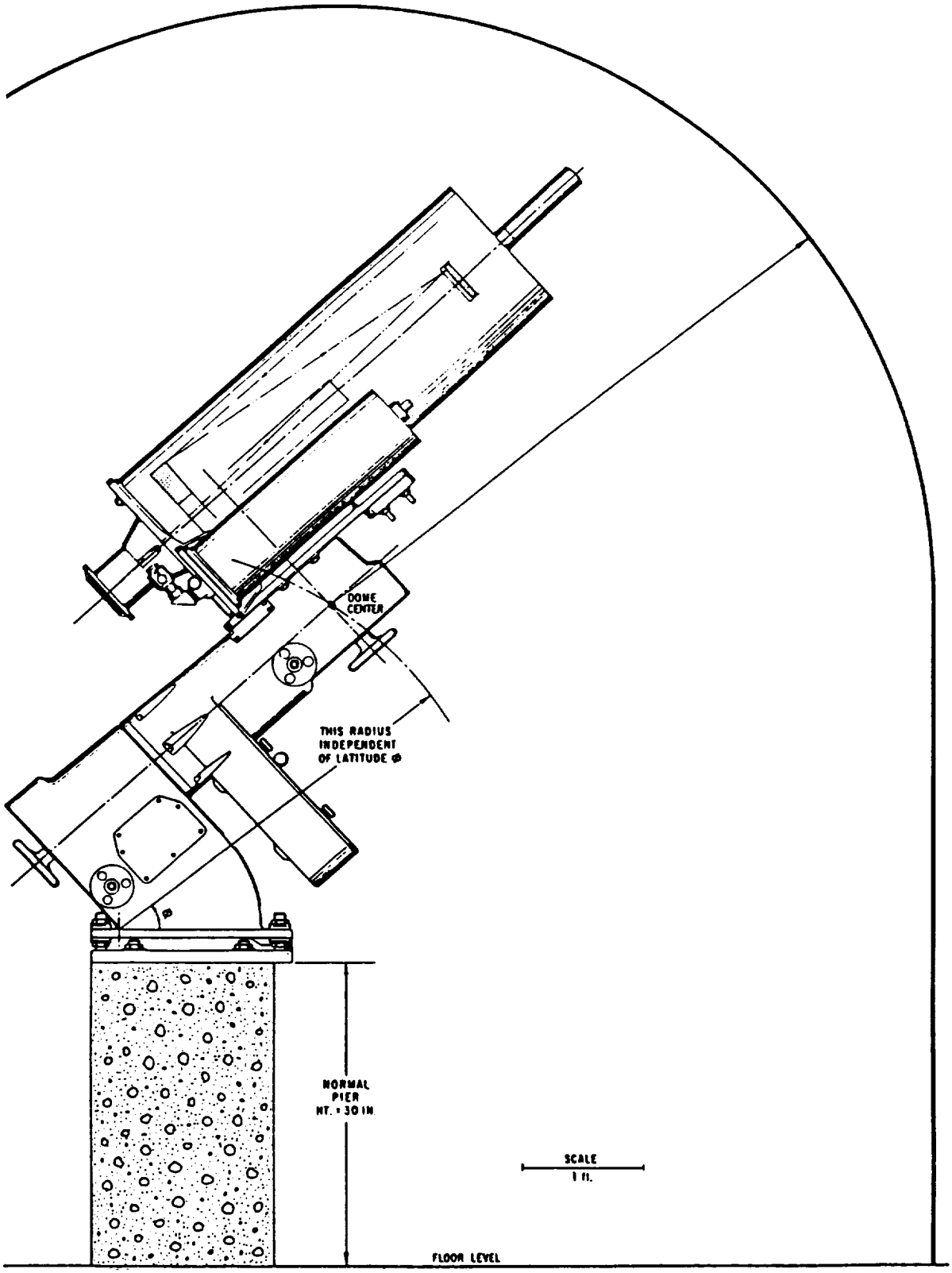

Figure 1. Schematic diagram of the MSFC Solar Vector Magnetograph telescope and mounting system.

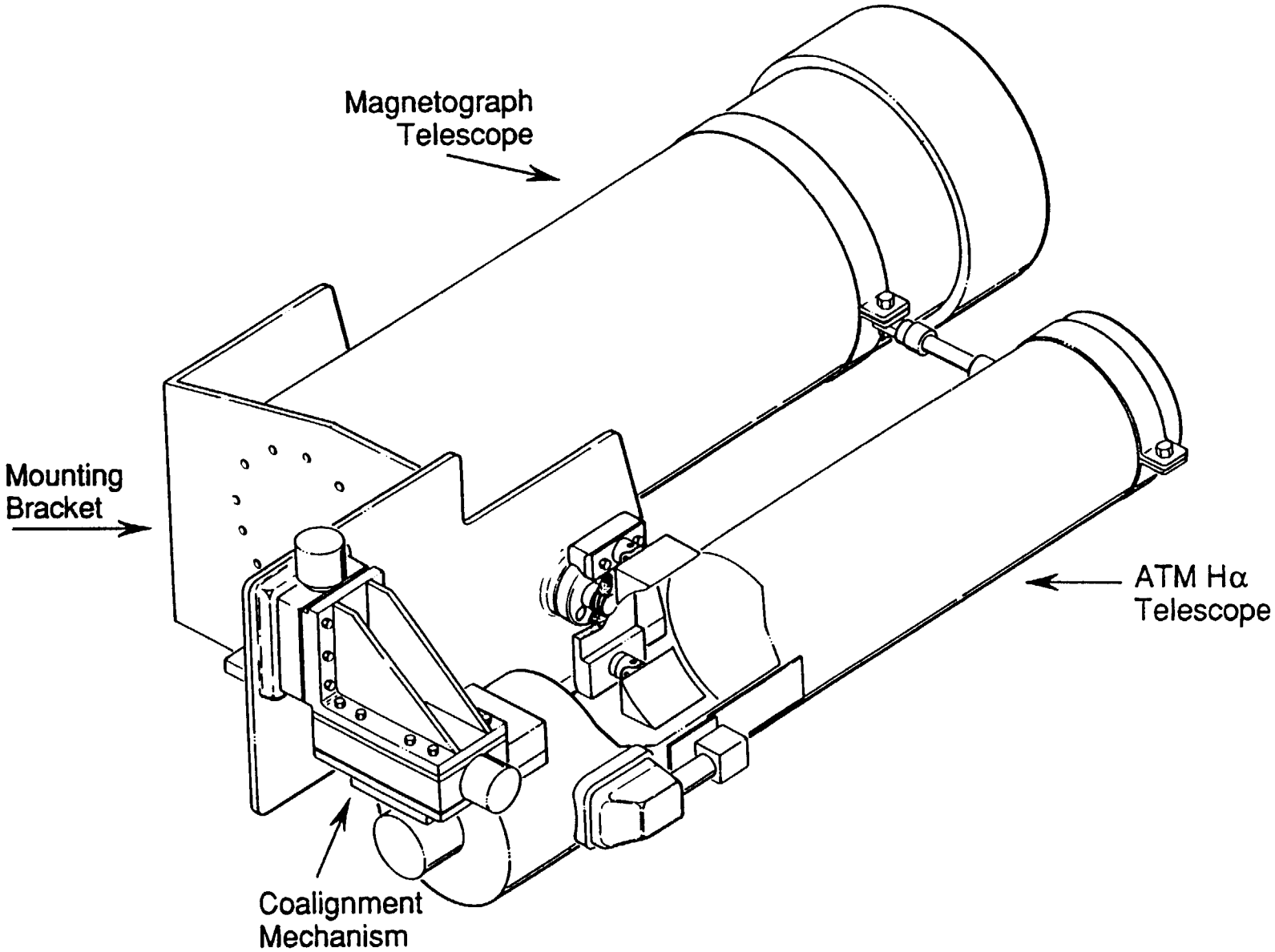

Figure 2. Final design for the coalignment mechanism and mounting bracket.

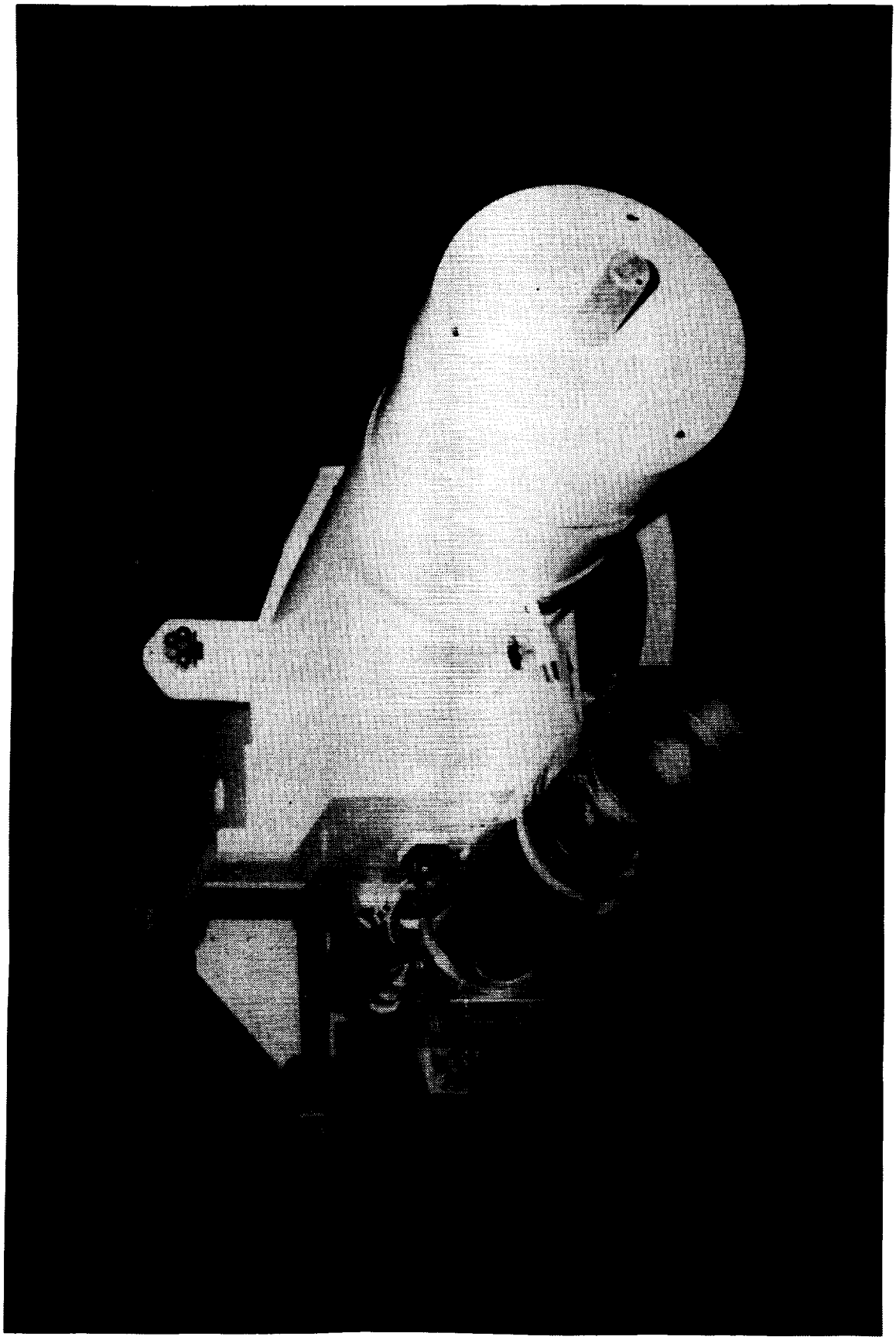

Figure 3. Front view of the MSFC Solar Vector Magnetograph coaligned with the Skylab/ATM Hα telescope.

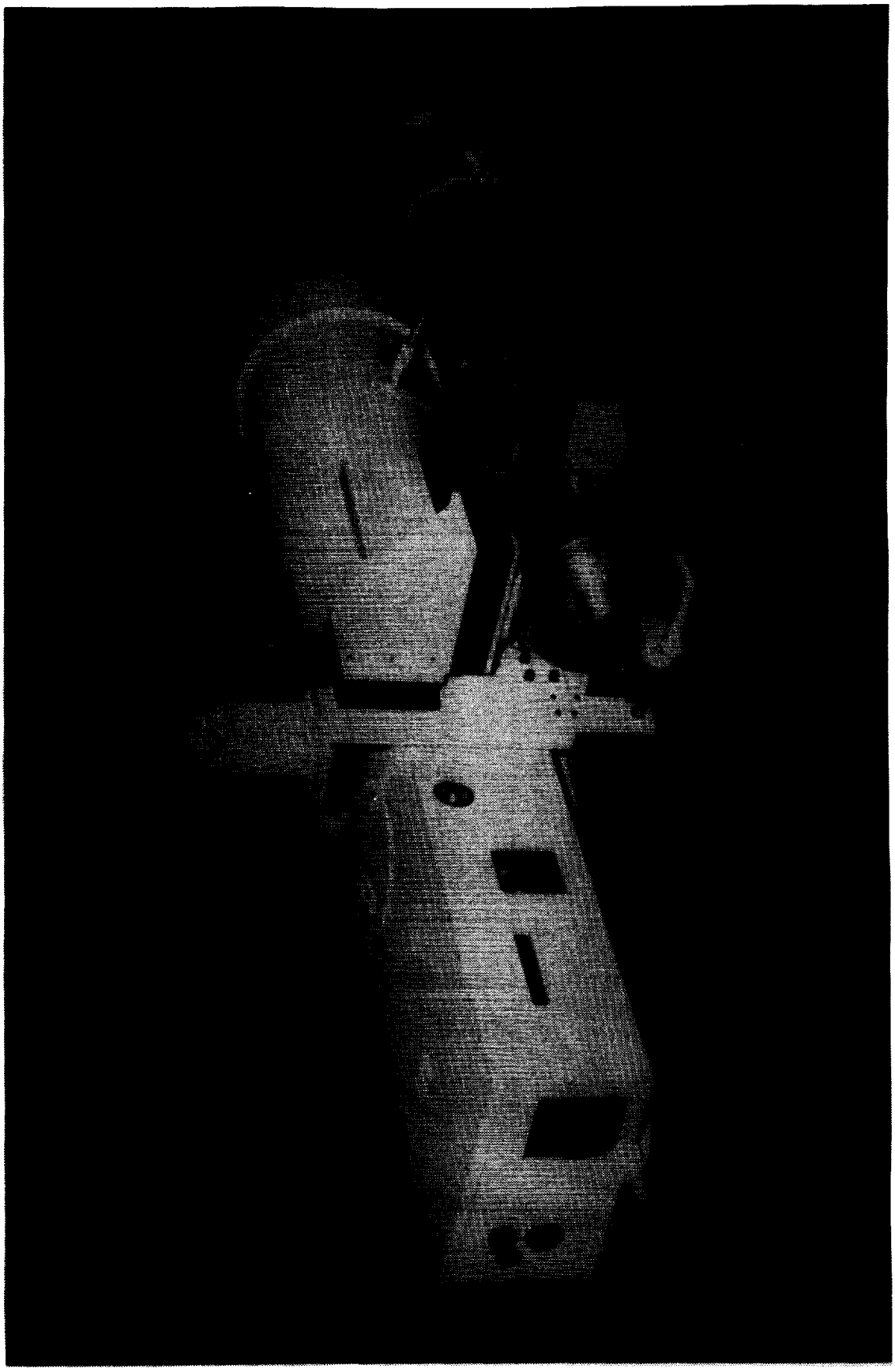

Figure 4. Rear view of the MSFC Solar Vector Magnetograph coaligned with the Skylab/ATM Hα telescope.

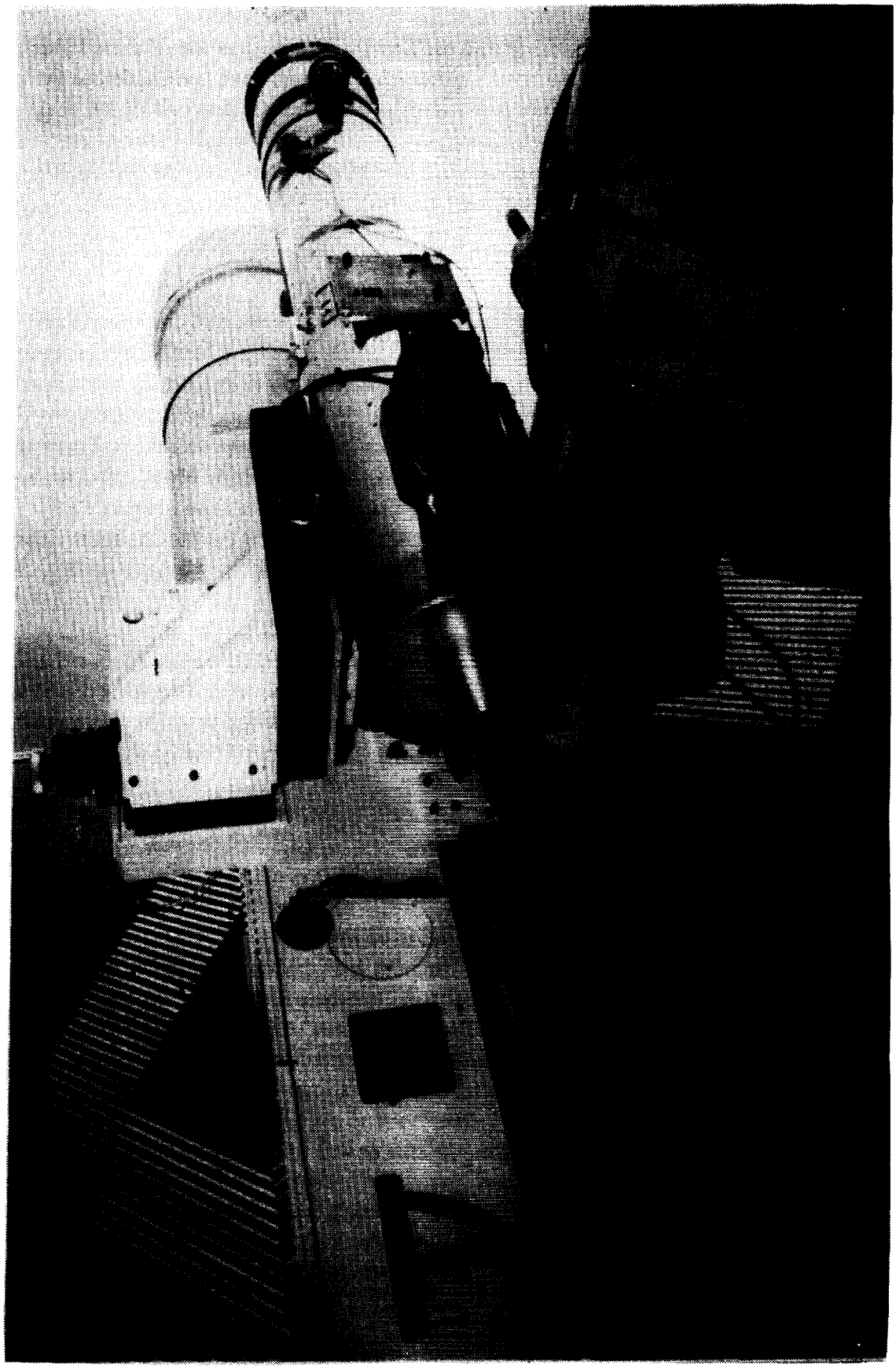

Figure 5. The MSFC Solar Vector Magnetograph and coaligned Skylab/ATM Hα telescope mounted at the MSFC Solar Observatory.

these cables can cause the guider system to go into oscillations. In anticipation of these kinds of problems, a motor-current monitor and an inverse time-delayed alarm have been added to the guider electronics to protect the guider motor when it operates at greater than half of the peak motor current for an extended period of time. Other modifications were made to the guider electronics to modernize the system; these included replacement of needle meters with LCD readouts and computer control of telescope pointing and focus.

4. VIDEO PROCESSING SYSTEM

Generation of movies from time-lapse images of the photospheric and chromospheric magnetic fields obtained with the coaligned instruments will add another scientific dimension to the MSFC Solar Vector Magnetograph program. The movies will allow us to study the dynamics of magnetic field configurations in solar active regions. Using the movies, we can detect small changes in the magnetic field that are associated with dynamic solar processes such as flares and differentiate them from the many small, uncertain variations that are usually observed. The movies will let us track all these variatons, compare them with variations seen in areas away from the solar activity, and thus determine if they are real changes using the hindsight provided by following their evolution over the extended time period of the movie.

To generate movies from the digital magnetograph data and video Hα images, we installed a video processor in the magnetograph's data analysis computer system, procured an RGB monitor for the display of images generated by the video processor, and integrated the Hα telescope's CCD video camera with a Sony 3/4" video recorder, UT video time generator, and a frame-code generator. We also procured an optical disk system to store the large amounts of magnetograph data needed to create movies.

The process of making a movie revolves around creating many sequential frames of images made up of magnetograms and Hα pictures. To do this, we interfaced the video processing system with a second, computer-controlled Sony video recorder to pick off a selected Hα image from the video tape and digitize it. The digitized image is scaled and coaligned with a corresponding (cotemporal) digital magnetogram, and both are displayed on the RGB monitor. The composite image is then stored in the computer and the process repeated on many subsequent sets of data until the complete set of observations has been processed. The video processor and Sony recorder are then used to record the sequential images on video tape. A schematic diagram of the video processing system is shown in Figure 6.

Procurement of the hardware for the video processor was only one of the tasks involved in this project; a major part of the work was development of software. A special program was developed for the vector magnetograph's computer to take repeated sequences of measurements as rapidly as possible. Software also had to be developed for the video processing, for registering, scaling, and coaligning images, for displaying combined images on the monitor, and for recording the images on video tape.

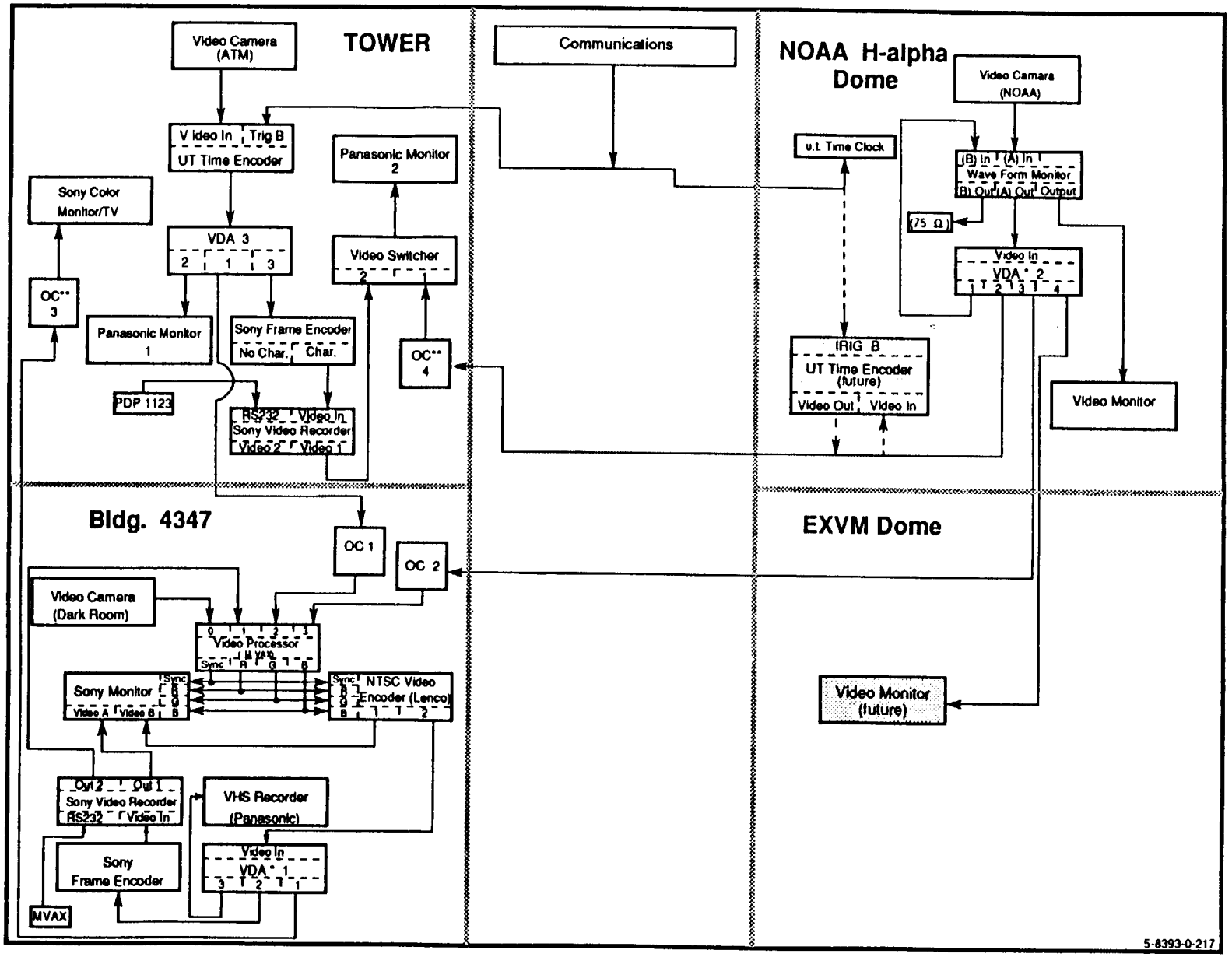

Figure 6. Schematic diagram showing the complete video processing system at the MSFC Solar Observatory.

5. INITIAL RESULTS

Observations with the coaligned Hα telescope and vector magnetograph have been underway since September 1989, and we have obtained some impressive and interesting data since then. Several major flares have been observed, including an M1/1N on October 15, 1989 and an X5/3B on October 24.[1] Reconfigurations in observed magnetic fields have also been correlated with Hα filaments, surges, brightenings, and subflares. In the following paragraphs, we will describe some of these observed events.

A. Flare of October 15

The October 15 flare started at 1430 UT, 6 minutes after the first MSFC vector magnetogram was obtained at 1424 UT. One component of the vector field (the component along the line-of-sight) is displayed in Figure 7a as contours, where solid (dashed) contours represent positive (negative) fields coming out of (going into) the photospheric surface. The points separating positive and negative fields mark the so-called magnetic "neutral line"; the major neutral line is indicated by the dark contour with numbers (1-127). The strongest fields are associated with the sunspots and are located in the areas of the highest positive contours (2500 G).

The image from the Hα telescope is shown in Figure 7b at the time of maximum flare area; the neutral line of the line-of-sight field in Figure 7a is superposed for reference. The central two areas of most intense emission of this flare are seen to lie on either side of the central segment of the neutral line. This orientation is typical: flare emission always straddles a portion of a magnetic neutral line in an active region.

In Figure 8a the other two components of the observed magnetic field vector are displayed as line segments; the orientation of the segments indicates the direction of the component transverse to the line-of-sight and the length denotes the intensity of that component. The major neutral line is again shown for comparison with Figure 7.

A magnetic field with the flux distribution exhibited by the line-of-sight component shown in Figure 7a can have different "energy states" depending on the distribution and configuration of the transverse component. The field with the lowest energy state is called a potential field since it is derived from a potential function and satisfies the Laplace equation with

---

[1] Flare radiation in x rays is measured on a logarithmic scale where C, M, and X denote peak fluxes at 1-8 Å of 10^{-3}, 10^{-2}, and 10^{-1} erg cm^{-2} sec^{-1}, respectively; X5 represents a peak flux of 5 x 10^{-1} erg cm^{-2} sec^{-1}. Flare area and optical intensity are qualitatively described by numbers (1-4, where 4 is the largest area) and symbols (F for faint, N for normal, B for bright), respectively.

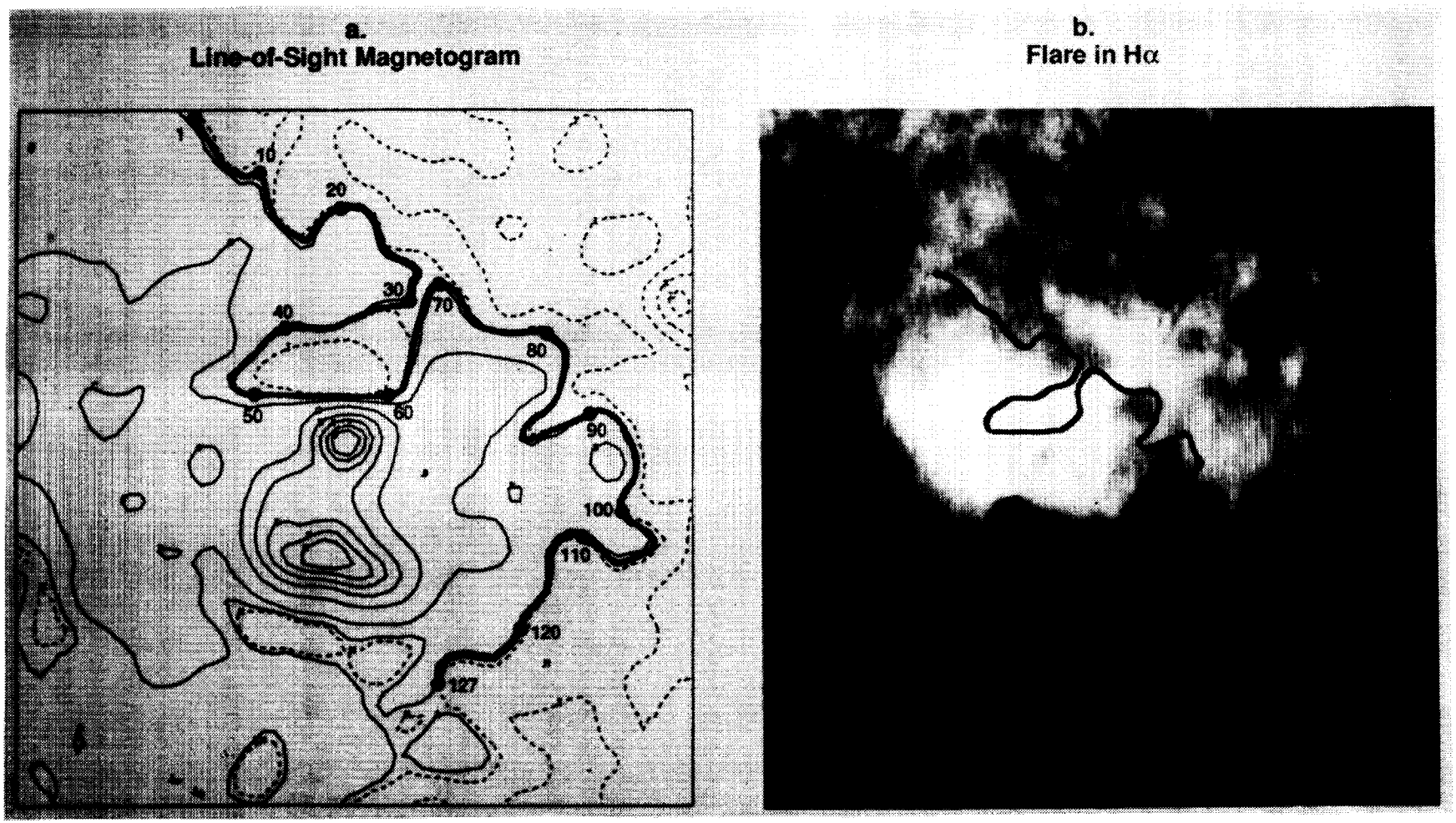

Figure 7. Images from the coaligned telescopes showing the photospheric magnetic field and chromospheric features in the region of a major solar flare. (a) Line-of-sight component of the magnetic field of a solar active region observed at 1424 UT on October 15, 1989. The numbered (dark) contour marks the magnetic "neutral" line where the line-of-sight field changes from positive (solid contours) to negative (dashed contours) polarity. (b) An Hα image of the solar flare that erupted in this active region at 1430 UT on October 15. The magnetic neutral line from Figure 7a is superposed on the Hα picture to indicate the location of the flare relative to the photospheric field.

the line-of-sight flux as boundary value. The transverse component of the potential field determined by the flux distribution of Figure 7a is shown in Figure 8b.

In comparing the observed and potential transverse fields along the segment of the neutral line straddled by the two central flare emissions (points 50 to 60 in Figure 7a), we see a particular signature of transverse fields at flare sites, the so-called "shear" of the field across the neutral line. The "shear" is understood to be the tendency of the transverse field to lie parallel to the magnetic neutral line rather than across it (the potential field configuration goes directly across from the positive to the negative side of the neutral line rather than being stretched parallel to it). This is a signature that was confirmed by observations with the MSFC vector magnetograph in the 1980's and placed on a quantitative basis for the first time by MSFC analyses [5,6]. This signature indicates that the magnetic field at the flare site is in a very nonpotential state and lends credence to theories in which the energy of a flare is derived from the magnetic energy of the field.

A quantitative analysis of this nonpotential state is shown in Figure 9 where we show the variation of the observed transverse field intensity B_T and angular shear $|\Delta\phi|$ along the major neutral line (points 1-127). By angular shear we mean the absolute difference between the orientations of the observed and potential transverse fields (the difference between the orientations of the line segments in Figures 8a and 8b). The significant point of this figure is that there is only one area where there is a coincidence of strong fields and large angular shear, points 50-60, and this is exactly where the two central flare emissions are seen - right where the field is the most nonpotential.

To illustrate more graphically this coincidence between the flare site and nonpotential fields, we show the line-of-sight field and neutral line in Figure 10 with points of strong fields and high shear indicated by the following two special symbols:

o $B_T \geq \frac{1}{2} B_T^{max}$ and $70° \leq |\Delta\phi| < 80°$,

■ $B_T \geq \frac{1}{2} B_T^{max}$ and $|\Delta\phi| \geq 80°$,

where B_T^{max} is the maximum field intensity along the relevant portion of the neutral line.

This "shear map" summarizes the quantitative analyses displayed in Figure 9 and visually displays them on the magnetic map of the active region. Such a map clearly indicates the areas of strongly nonpotential magnetic fields and provides a straightforward visual comparison with the locations of the flare emissions seen in the coaligned Hα image. This comparison leaves little doubt in this instance that the flare was located where the magnetic field was in its most nonpotential state.

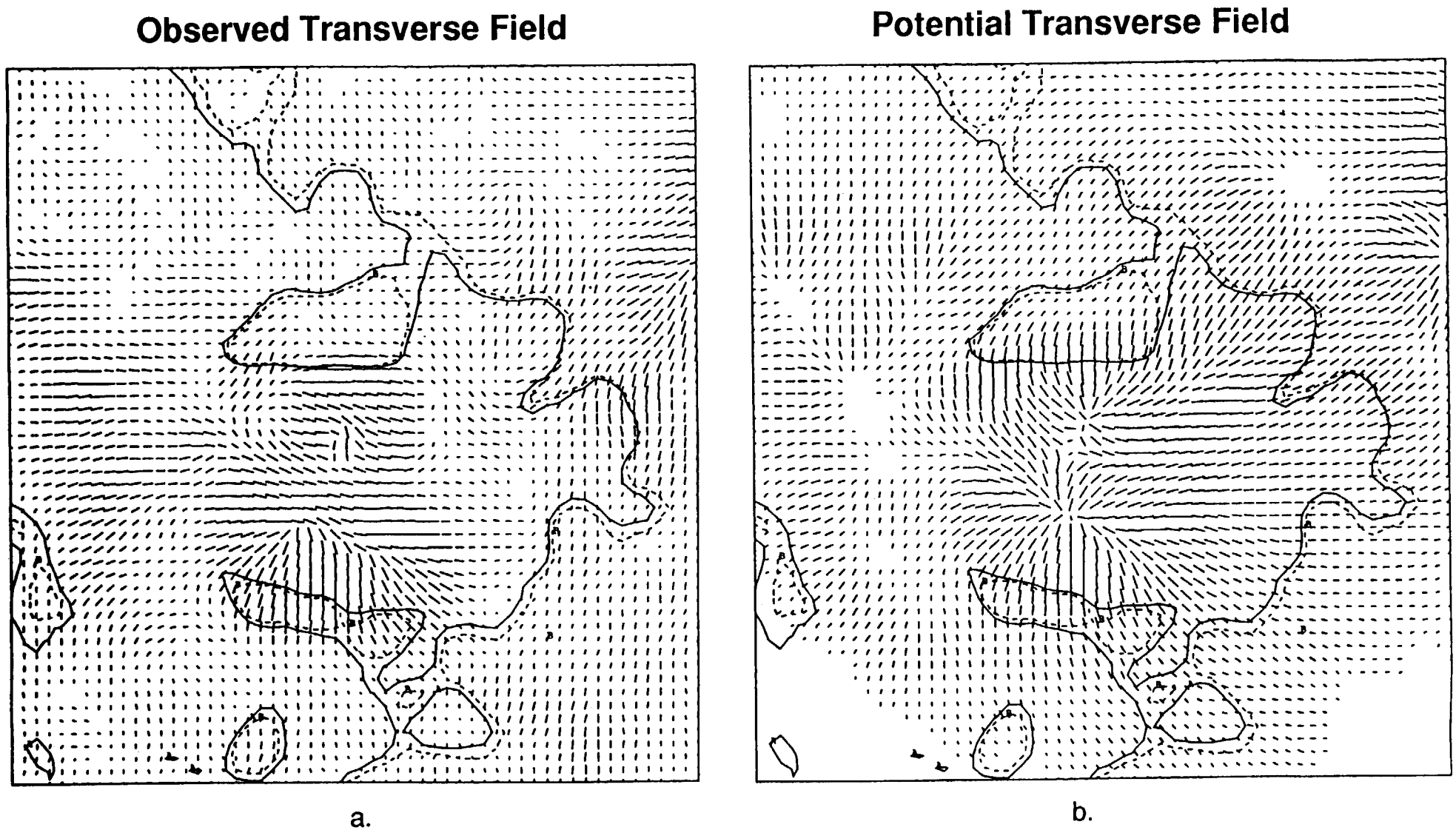

Figure 8. Transverse magnetic fields in the flaring active region. (a) The observed transverse field is displayed in strength and direction by the length and orientation, respectively, of the line segments. (b) The transverse component of the potential field for this region. The magnetic neutral line is indicated in both (a) and (b) for reference with Figure 7.

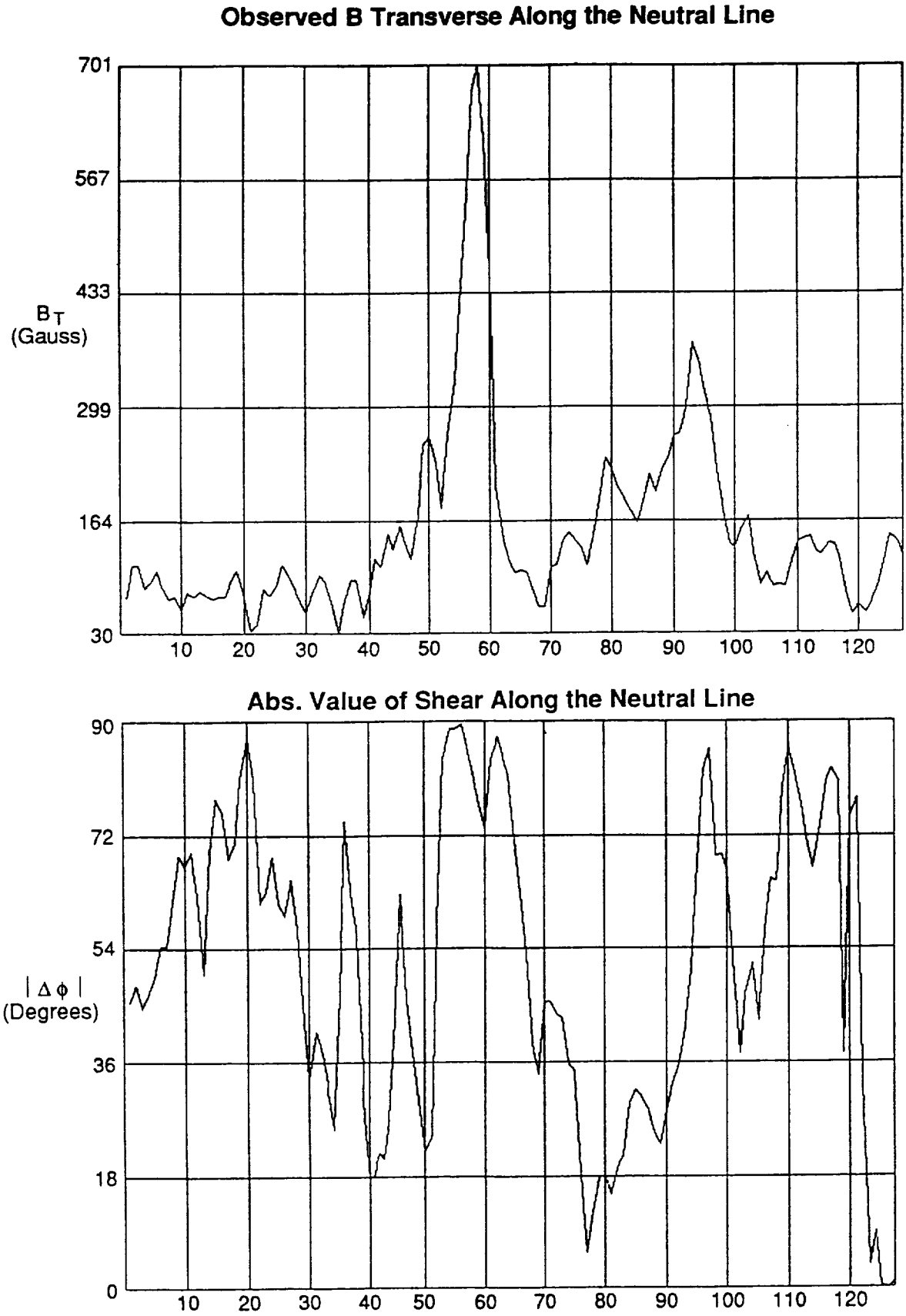

Figure 9. Quantitative analysis of the nonpotential characteristics of the magnetic field along the magnetic neutral line in the flaring region. The top panel shows the variation of the observed field strength along the magnetic neutral line. The lower panel shows the variation of angular shear along the neutral line. The points along the neutral line refer to the numbered pixels in Figure 7a.

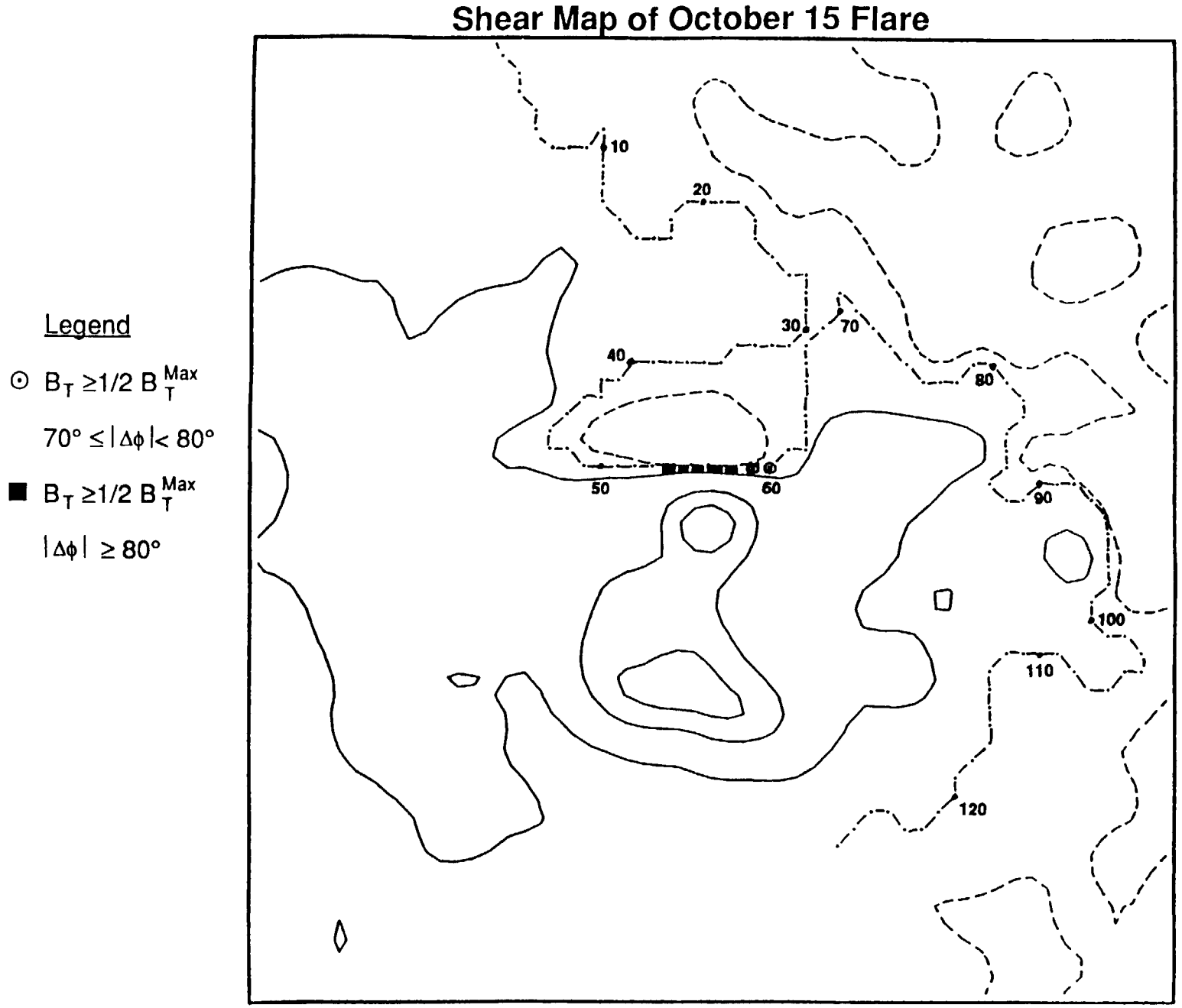

Figure 10. Shear map for the flaring active region. The circles mark sites of strong fields and large angular shear; the filled squares mark sites of strong fields and the largest angular shear. The solar flare was observed in the area marked by the circles and squares.

B. The X5/3B Flare of October 24

An Hα image of the big flare on October 24 is shown in Figure 11. For this flare the magnetic field configuration was difficult to analyze since the active region was very close to the western limb of the Sun where foreshortening effects compress the spatial scale *and* projection effects intermingle the three components of the magnetic field. (The *measured* components of the magnetic vector are along the line-of-sight and perpendicular to the line-of-sight. At the center of the Sun, the component along the line-of-sight is perpendicular to the solar surface, whereas at the edge of the Sun, this component is tangent to the surface.)

C. Filament Fields

The importance of having coaligned, cotemporal magnetograms and Hα images is borne out from an analysis of observations obtained during the period October 28-30, 1989. Our analysis has shown reconfigurations of the magnetic field going hand in hand with changes in filament structures in an active region. On October 28, a filamentary feature was observed to run parallel to the measured transverse magnetic field. The Hα image recorded at 1942 UT on this date is seen in Figure 12, and the magnetic field observed at 1933 UT is shown on the overlay. The line-of-sight component of the magnetic field is displayed by contours (±25, 500, 1500 G), and the transverse component is indicated in magnitude and orientation by the length and direction, respectively, of the line segments (transverse fields less than 150 G are not displayed). The transverse field is seen to extend from the leader sunspot eastward (toward the bottom of the figure) to the small following spots located in the trailing area of negative polarity. The Hα image shows a filamentary feature lying along this transverse field. On the succeeding day, realignments are seen in the magnetic field and the filament is no longer visible in the Hα image. Figure 13 shows the Hα image at 1620 UT on October 29; the field configuration observed at 1627 UT is shown on the overlay. Now the transverse field east of the main leader spot is seen to turn into the plage area and does not extend to the small trailing spots as it did on the 28th. Figure 14 shows the Hα image taken at 1509 UT on October 30 with the vector magnetogram at 1610 UT overlaid. The major change now is the growth of the field in the area of a developing sunspot of negative polarity just east of (below) the magnetic neutral line.

D. Sub-Flare and Surge at a Site of Field Reconfiguration

After only 10 months of operation, we have found in a number of instances that the Hα observations show phenomena that pinpoint subtle reconfigurations in the magnetic field that would probably have been missed in analyses of vector magnetograms before coaligned Hα images were available. Such is the case in observations on June 12 and 13, 1990, of AR 6100. On June 12 our attention was focused on the magnetic field along the major neutral line lying to the east of the main negative-polarity spot; this neutral line is indicated by the dark contour in the line-of-sight magnetogram shown in Figure 15a. The reason for this interest is seen from an inspection of the transverse component of the field in Figure 15b; the field along the southern (right side in the figure) part of the neutral line exhibits the "sheared" configuration that so often

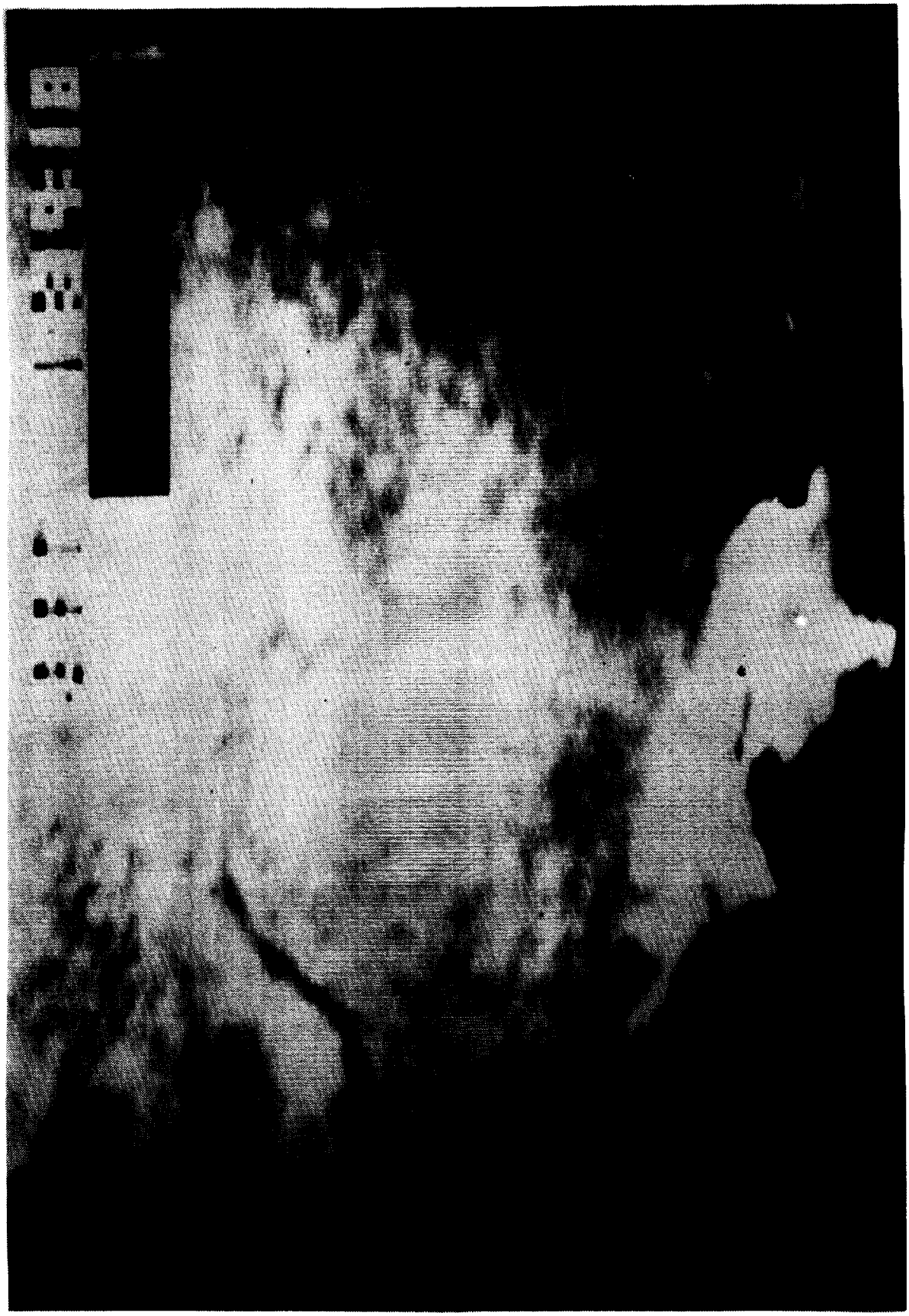

Figure 11. Hα picture of the X5/3B flare of October 24, 1989.

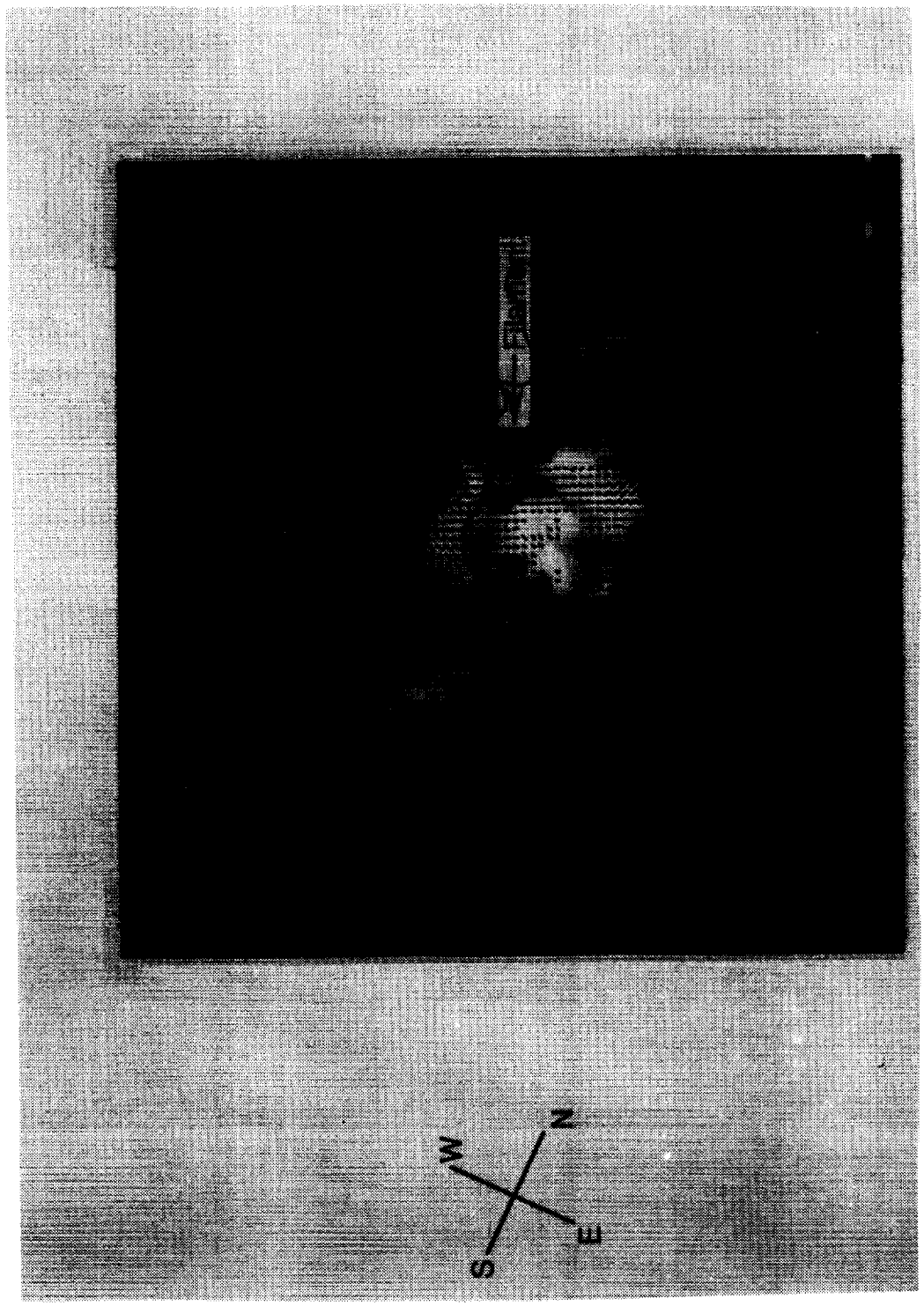

Figure 12. MSFC vector magnetogram and Hα image for an active region observed on October 28, 1989. The filamentary feature below the sunspot is seen to be aligned with the transverse magnetic field.

Figure 13. MSFC vector magnetogram and Hα image taken on October 29, 1989. The transverse magnetic field below the sunspot has changed configuration and the filamentary feature seen on the previous day is no longer visible.

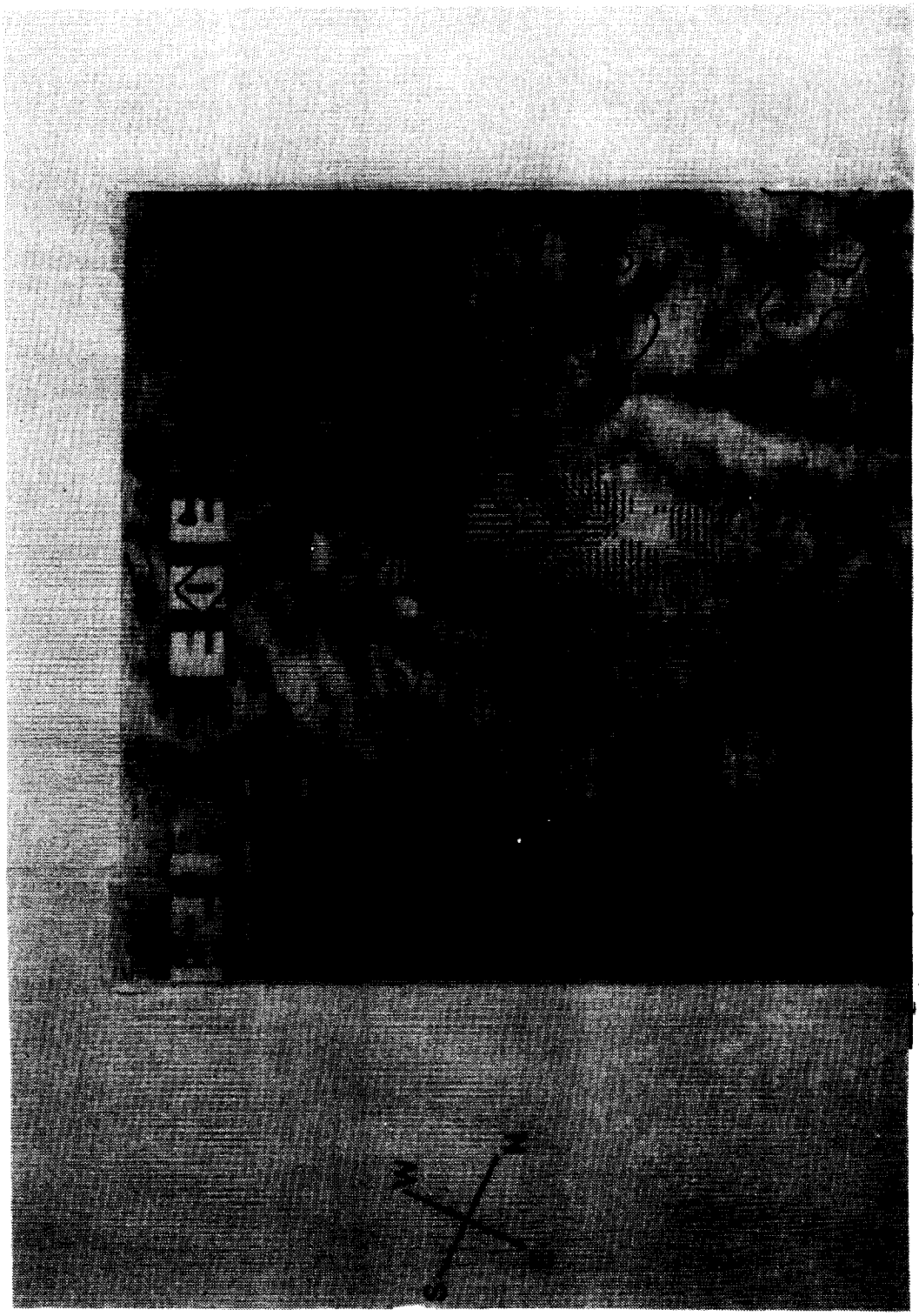

Figure 14. MSFC vector magnetogram and Hα image taken on October 30, 1989. Field reconfigurations continue with the development of another sunspot in the region.

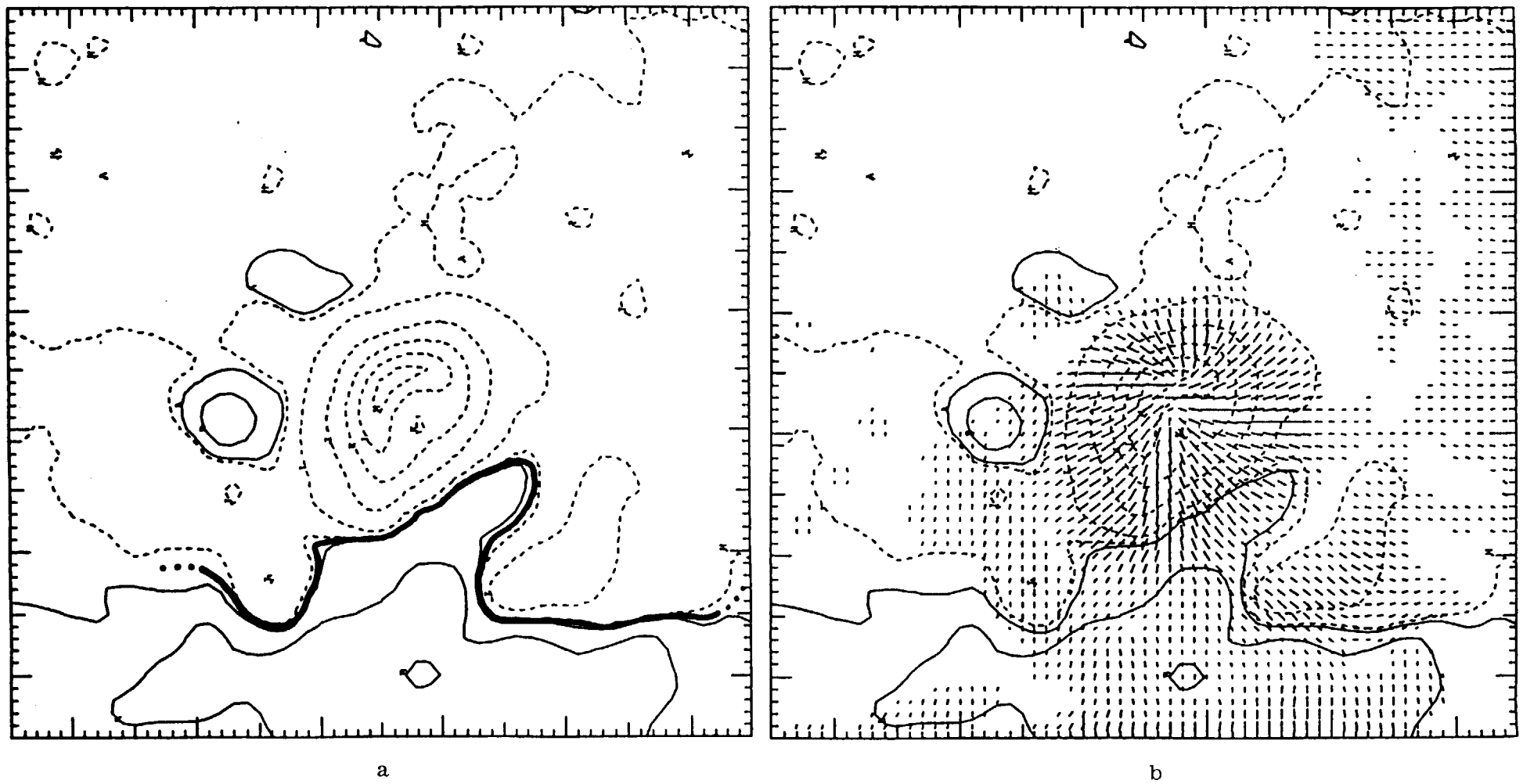

Figure 15. Magnetic field of active region AR 6100 observed at 1339 UT on June 12, 1990. (a) Line-of-sight magnetogram with the major magnetic neutral line indicated by the dark contour. (b) Transverse component of the magnetic field (line segments) superposed on the line-of-sight component (contours).

heralds the onset of major flares. The isolated positive polarity just to the north (left) of the main spot in Figure 15 was largely ignored in our analysis of the data on that day. Indeed, this isolated polarity seemed to decrease in magnetic intensity the following day, June 13, as seen in the line-of-sight magnetogram in Figure 16a. Again, attention was centered on the sheared configuration along the southern part of the neutral line (seen in Figure 16b) which was as pronounced as on the previous day.

However, on the 13th the seemingly "benign" isolated polarity was the site of the dynamic sequence of events recorded with the Hα video system and shown in Figure 17. In Figure 17a there is only a small enhanced emission seen in Hα at 1514 UT, but at 1636 UT a sub-flare was in progress (Figure 17b). Following the onset of the flare, surging material was observed at 1643 UT (Figure 17c), and this continued for several hours (Figure 17d at 1859 UT).

A re-examination of the magnetic field in this area readily uncovered the source of these dynamic events: the field in this area had transformed literally overnight from a ~ potential to a nonpotential configuration. In Figure 18a, an enlargement of the magnetogram for June 12 (Figure 15b) indicates that the transverse field direction at the magnetic neutral line (between the solid and dashed contours in the shaded area) was oriented more or less as a potential field would be, going from the positive, isolated polarity across the local neutral line toward the main negative spot. The corresponding enlargement in Figure 18b for the observations on June 13 shows that the transverse field direction along the neutral line was aligned parallel to the neutral line in a sheared configuration.

While this reconfiguration was very subtle, its coincidence with the dynamic events that took place makes us certain that it was a real change and that it was most probably the underlying cause of the flare and surge. But without the coaligned observations from the Hα system, this cause and effect connection would most certainly have been missed.

E. Movies of Coaligned Images

The next obvious step beyond examining individual sets of data on different days is to generate movies of the coaligned observations. Although some software still must be developed before we realize the full potential of producing movies from these data, the concept of generating movies *has been verified.* Using observations of the vector magnetic field obtained in March 1988, we borrowed a μVax computer, developed the necessary software, and produced a movie that was presented at the June 1988 meeting of the American Astronomical Society in Kansas City [7].

6. SUMMARY

With the conclusion of this Center Director's Discretionary Fund program, MSFC solar scientists have realized a long-awaited goal to observe simultaneously the magnetic field in the photosphere and chromosphere of the Sun. With this enhanced capability, the MSFC Solar

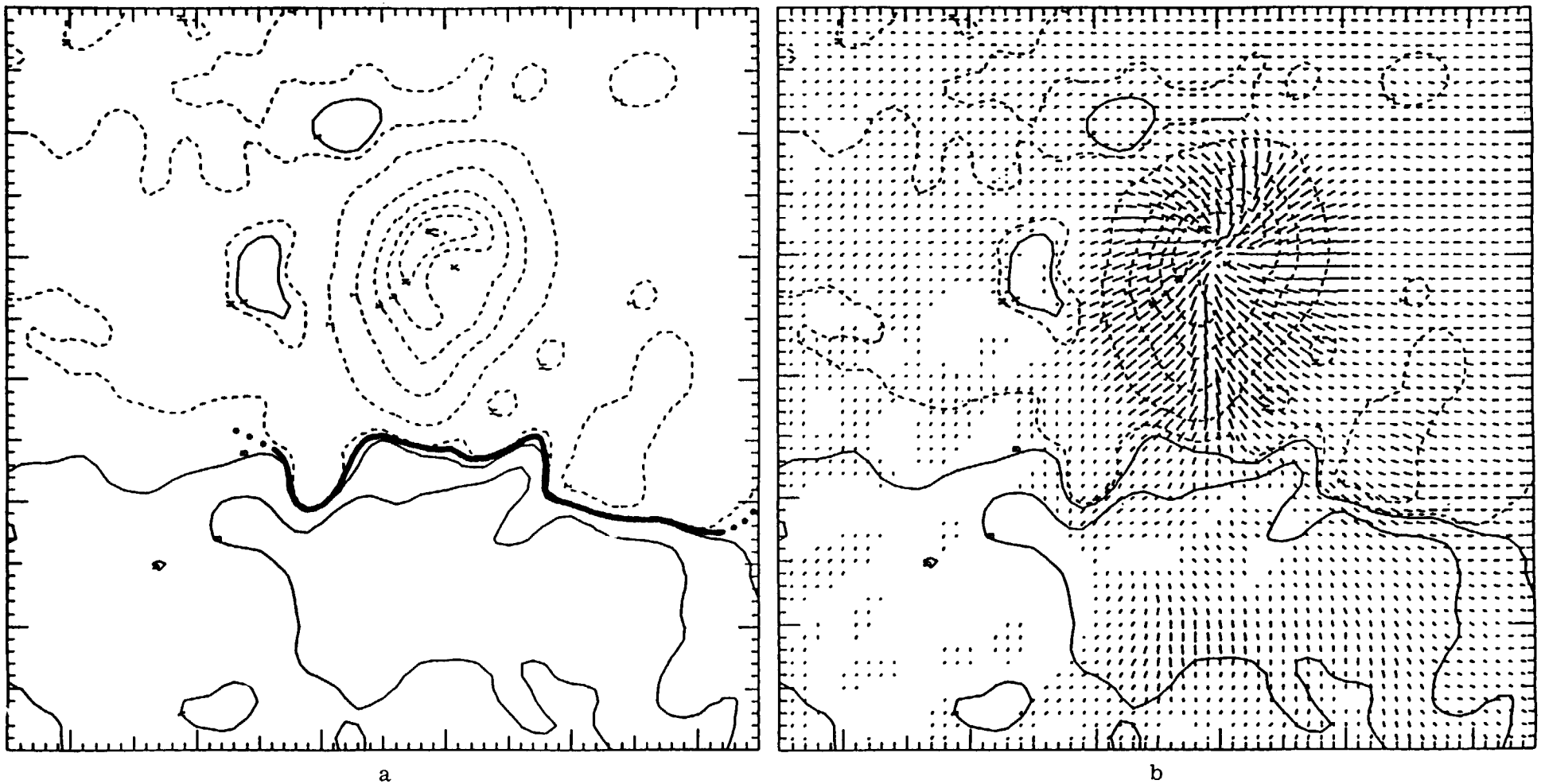

Figure 16. Magnetic field of active region AR 6100 observed at 1524 UT on June 13, 1990. (a) Line-of-sight magnetogram with the major magnetic neutral line indicated by the dark contour. (b) Transverse component of the magnetic field (line segments) superposed on the line-of-sight component (contours).

ORIGINAL PAGE
BLACK AND WHITE PHOTOGRAPH

Figure 17. Sequence of Hα images showing development of sub-flare and surge on June 13, 1990. (a) Pre-flare at 1514 UT. (b) Sub-flare at 1638 UT. (c) Surge at 1643 UT. (d) Surge at 1859 UT.

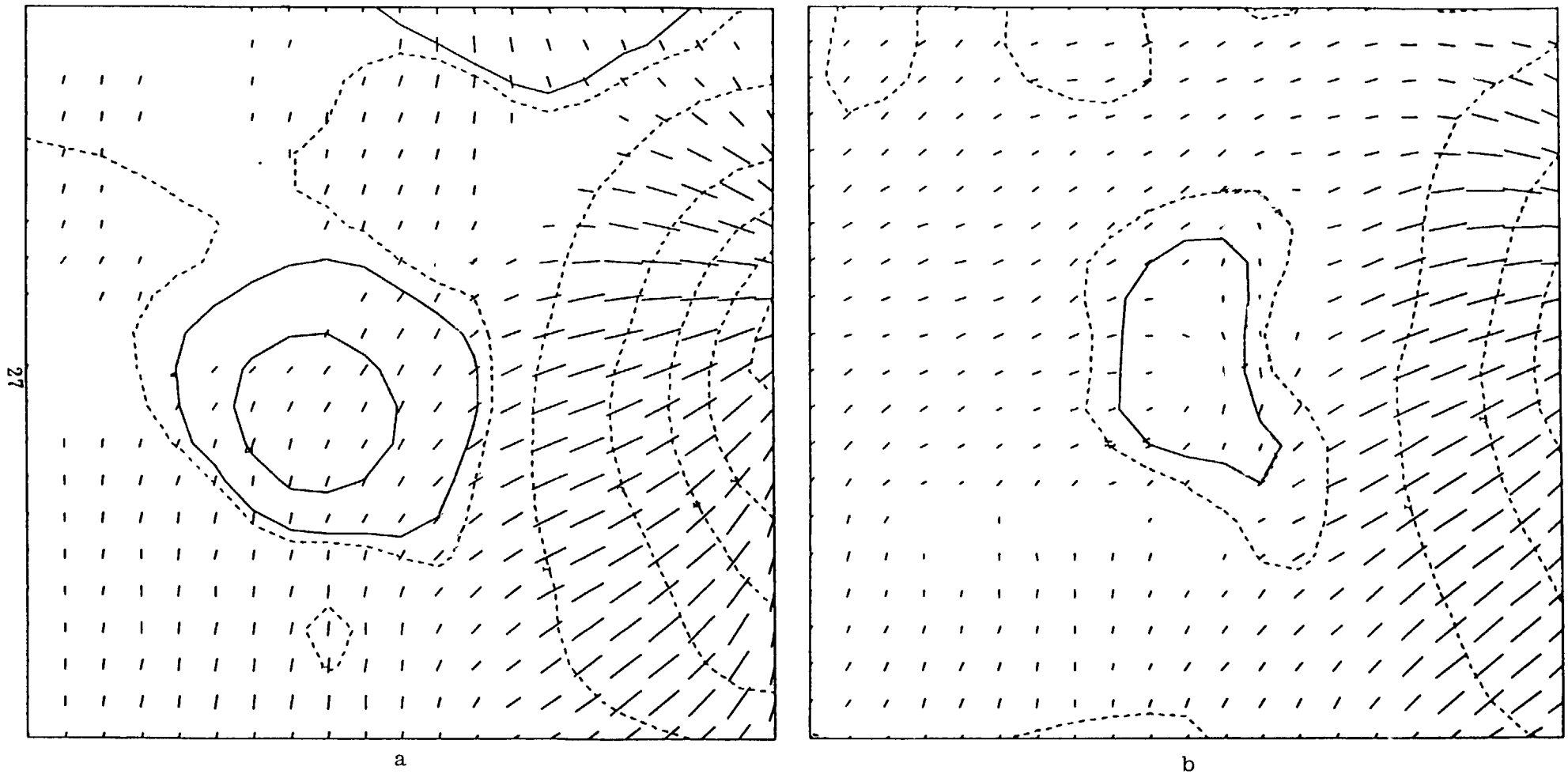

Figure 18. Observed reconfiguration of magnetic field prior to the sub-flare and surge activity on June 13, 1990. (a) Enlargement of the vector magnetic field observed at 1339 UT on June 12 in the vicinity of an isolated positive-polarity field. The transverse field direction is seen to make an angle with the magnetic neutral line of approximately 45° (shaded area). (b) The same area observed at 1524 UT on June 13. Now the transverse field in the vicinity of the isolated polarity lies parallel to the magnetic neutral line (shaded area), an orientation that is highly nonpotential.

Observatory will continue to support NASA space science missions, conduct benchmark research, and remain at the forefront of research in solar magnetic fields.

As the results presented in this report demonstrate, the coaligned observations from the two telescopes have already led to significant discoveries. In particular, our capabilities for flare research have been substantially improved with the combination of the shear analysis from the photospheric vector field and the coaligned image of the flare in the chromosphere. By studying the correlation of magnetic shear and flares, we expect to develop a better theoretical understanding of the flare process; such an understanding will be essential to the development of techniques to accurately predict when and where major solar flares will erupt. These flare predictions will become necessary as the Agency enters into the era of manned missions to Mars and manned Lunar bases.

REFERENCES

[1] M. J. Hagyard, N. P. Cumings, E. A. West, and J. E. Smith: The MSFC Vector Magnetograph, Solar Phys. **80** (1982), p. 33.

[2] M. J. Hagyard, N. P. Cumings, and E. A. West: The New MSFC Solar Vector Magnetograph, in Proceedings of Kunming Workshop on Solar Physics and Interplanetary Travelling Phenomena, C. deJager and Chen Biao, eds., Science Press (1985), p. 204.

[3] M. J. Hagyard, E. A. West, and N. P. Cumings: The New MSFC Solar Vector Magnetograph, NASA Technical Memorandum 82568 (1984).

[4] J. F. Markey and R. R. Austin: High Resolution Solar Observations: the Hydrogen-Alpha Telescopes on Skylab, Applied Optics **16** (1977), p. 917.

[5] M. J. Hagyard, J. B. Smith, Jr., D. Teuber, and E. A. West: A Quantitative Study Relating Observed Shear in Photospheric Magnetic Fields to Repeated Flaring, Solar Phys. **91** (1984), p. 115.

[6] M. J. Hagyard and D. M. Rabin: Measurement and Interpretation of Magnetic Shear in Solar Active Regions, Adv. Space Res. **6**(6) (1986), p. 7.

[7] E. A. West, M. J. Hagyard, and G. A. Gary: Development of an Image Processing System to Study Changes in Coaligned Vector Magnetograms and Hα Images, Bulletin Am. Astron. Soc. **20**(2) (1988), p. 711.

APPROVAL

COALIGNED OBSERVATIONS OF SOLAR MAGNETIC FIELDS AT DIFFERENT HEIGHTS: MSFC CENTER DIRECTOR'S DISCRETIONARY FUND FINAL REPORT (PROJECT NUMBER 88-10)

By M. J. Hagyard, E. A. West, G. A. Gary, and J. E. Smith

The information in this report has been reviewed for technical content. Review of any information concerning Department of Defense or nuclear energy activities or programs has been made by the MSFC Security Classification Officer. This report, in its entirety, has been determined to be unclassified.

E. TANDBERG-HANSSEN
Director
Space Science Laboratory

☆ U.S. GOVERNMENT PRINTING OFFICE 1990—531—081/20227

ACKNOWLEDGEMENTS

The investigators would like to acknowledge the contributions of the many individuals and organizations that have made this CDDF project so successful. We particularly wish to thank John Gibson and Bob Raney (EP63) for their efforts in designing the coalignment system, and special thanks are due Mr. Gibson for his work throughout the project, especially in coordinating the fabrication of the mounting brackets in the MSFC Machine Shop. The modifications to the guider electronics were ably carried out by Monty Montenegro (EB24), and assistance in developing some of the video processing software was provided by Hugh Zeanah (formerly of EB44). Fabrication of the mounting brackets and other necessary components was done by the MSFC Machine Shop under the direction of the Fabrication Division of EH Laboratory. We are very grateful to Hank Moeller of Perkin-Elmer for all his assistance in helping us understand the ATM Hα telescope system. Finally, we express our appreciation to the Center Director's Discretionary Fund program for making this project a reality.

NASA

Report Documentation Page

1. Report No.	2. Government Accession No.	3. Recipient's Catalog No.
NASA TM- 103516		

4. Title and Subtitle	5. Report Date
Coaligned Observations of Solar Magnetic Fields at Different Heights--MSFC Center Director's Discretionary Fund Final Report (Project Number 88-10)	September 1990
	6. Performing Organization Code: ES52

7. Author(s)	8. Performing Organization Report No.
M. J. Hagyard, E. A. West, G. A. Gary, and J. E. Smith	10. Work Unit No.

9. Performing Organization Name and Address	11. Contract or Grant No.
George C. Marshall Space Flight Center Marshall Space Flight Center, AL 35812	13. Type of Report and Period Covered: Technical Memorandum

12. Sponsoring Agency Name and Address	14. Sponsoring Agency Code
National Aeronautics and Space Administration Washington, D.C. 20546	

15. Supplementary Notes

Prepared by Space Science Laboratory, Science & Engineering Directorate.

16. Abstract

This document constitutes the final report for MSFC Center Director's Discretionary Fund Project Number 88-10. The objective of this program was to develop the capability for obtaining cotemporal and coaligned observations of the structure and evolution of the Sun's magnetic field at two different heights in the solar atmosphere: the photosphere, which is the lowest region observable with optical telescopes, and the chromosphere, which lies just above the photosphere and is a region where the magnetic field dominates the gas motions so that a well-ordered structure governed by the field is observed. By obtaining this three-dimensional picture of the solar magnetic field, we can develop a better understanding of the magnetic forces that produce and control the dynamic, high-energy phenomena occurring in the solar atmosphere that can affect the entire heliosphere, including our own terrestrial environment.

17. Key Words (Suggested by Author(s))	18. Distribution Statement
Solar Magnetic Fields, Chromospheric Field Structure, Photospheric Vector Field	Unclassified--Unlimited

19. Security Classif. (of this report)	20. Security Classif. (of this page)	21. No. of pages	22. Price
Unclassified	Unclassified	37	NTIS

NASA FORM 1626 OCT 86

For sale by the National Technical Information Service, Springfield, VA 22161-2171